The 14th International Topical Meeting on Nuclear Reactor Thermalhydraulics, NURETH-14
Toronto, Ontario, Canada, September 25-30, 2011

NURETH14-106

REYNOLDS AVERAGED NAVIER-STOKES (RANS) AND LARGE EDDY SIMULATIONS (LES) OF THE AIR-WATER TOPFLOW-PTS EXPERIMENT

B. Niceno[1], T. Lumpp[1], P. Apanasevich[2] and D. Lucas[2]
[1] Paul Scherrer Institut, Villigen, Switzerland
[2]Helmholtz-Zentrum Dresden-Rossendorf, Dresden, Germany

Abstract

The occurrence of a PTS in a reactor vessel is an important phenomenon for assessing nuclear reactor safety. New experiment was conducted at HZDR, focused on thermal mixing processes in the cold leg and the downcomer of two-phase PTS case. Present work reports CFD analysis of steady-state air-water case. CFD analysis was conducted with two turbulence-modeling approaches, RANS and LES. Multiphase situation was modeled with VOF approach. Simulations were performed using the ANSYS Fluent 12 package. Comparison of computed temperatures results and measurements along the thermo-couple lines revealed results depend on the turbulence model used.

Introduction

The occurrence of Pressurized Thermal Shock (PTS) in a reactor vessel is an important phenomenon for assessing nuclear reactor safety. The phenomenon is triggered by the injection of cold Emergency Core Cooling (ECC) water into the cold leg. The cold water mixes with the hot coolant present in the cold leg causing thermal stratification which may reach the downcomer. The capabilities to model PTS with CFD methods were assessed within the NURESIM project [1] on separate effect tests [2-5], and it was concluded that further Computational Fluid Dynamics (CFD) model improvements are needed to achieve reliable prediction [6-7]. To that end, a new experiment was designed and conducted at HZDR [8]. The experimental programme is financed by a consortium in which PSI and HZDR are members. The focus of the new experiment is the thermal mixing processes in the cold leg and the downcomer of the stratified two-phase PTS case. Two cases were considered experimentally, air-water and steam-water.

Currently available CFD tools are not able to simulate accurately all phenomena that occur in the cold leg and the downcomer during the ECC injection. Numerical simulations have already been performed with moderate success; see e.g. [5, 9-11]. In the frame of the EU project NURISP (Nuclear Reactor Integrated Simulation Project) attempts are made to improve the CFD modelling for two-phase PTS situations. For this purpose, two reference cases out of the TOPFLOW-PTS experimental programme were defined: one for steady air-water and one for steady steam-water flow. The NEPTUNE_CFD code [13] as well as the ANSYS CFX [14] and FLUENT [15] codes are used in the project for PTS investigations.

This work, which is a result of our involvement in the EU project NURISP, reports a CFD analysis of the steady-state air-water case and the comparison with experimental data at certain points. The case considered has no mass transfer at the interface, and its main purpose is to assess the performance of difference turbulence modelling approaches. We conduct CFD analysis with two turbulence modelling approaches, RANS and LES. The RANS cases were performed with k-ε and

SST models, while LES was performed using Smagorinsky and the dynamic sub-grid scale models. In all cases, the near-wall region is modelled by a wall function. All simulations were performed on the same strictly hexahedral grid with slightly more than 850,000 cells. The multiphase situation was modelled using the Volume Of Fluid (VOF) approach. All simulations were done in unsteady mode, making the difference in CPU time between RANS and LES less pronounced than usual. Simulations were performed using the ANSYS Fluent 12 package. Comparison of computed temperatures results and measurements along the thermo-couple lines in the cold leg and the downcomer, revealed that temperatures in the water can be well predicted by all models.

The paper is divided in two parts. In the first part, physical models, computational domain, boundary and initial conditions, as well as numerical scheme are described. The discussion of the results will be described in the second part. Geometry of the TOPFLOW-PTS experimental setup, as well as the measurement and computational results are reported in non-dimensional form here, due to confidentiality agreement with the TOPFLOW-PTS consortium.

1. Numerical simulations

1.1 Mathematical models

ANSYS Fluent 12.0 has been used to integrate the governing equations. The Volume Of Fluid (VOF) approach was used to simulate the multiphase situation. The VOF describes the interface between the phases as a set of polygons spanned over the numerical mesh. One set of Navier-Stokes conservation equations is used for the entire system, with corresponding physical properties for each of the working fluids. In addition to the momentum and energy conservation equations, jump conditions at the interface between the fluids must be prescribed, e. g. surface tension and mass transfer. In present work there is no mass transfer between the fluids. Furthermore, surface tension is neglected, due to small curvatures of the interfaces in the entire computational domain.

Turbulence was modeled by RANS and LES approaches, and the influence of the turbulence model on the computed results is the main focus of this work together with the comparison with experimental results. In the RANS approach, governing equations are averaged in time, leading to occurrence of additional stress terms which are unknown and must be modeled. The variety of RANS models is immense, but this work focuses on two models: k-ε and Shear Stress Transport (SST). The k-ε model is undoubtedly the most widely spread model in industry mainly due to its robustness. The SST model is essentially a combination of the k-ε model, which behaves well far from the walls, and k-ω model, which behaves better close to the wall.

In LES, on the other hand, governing equations are averaged over regions of space. The space averaging in LES is referred to as “filtering”. In the framework of the finite volume method, used to discretize the governing equations in the present work, filtering is performed over control volumes, i.e. cells of the numerical grid. The value computed in each of the cell centers is the filtered value. The filtering, however, gives rise to additional stresses similar to the ones occurring from time-averaging, but with a different physical interpretation. In case of LES, the additional stresses come from sub-grid-scale (SGS) motions, i.e. structures smaller than the grid size. Since it is generally assumed that these SGS motions are less energetic than the grid scale ones, more homogeneous and not specific to a particular flow configuration, SGS models should be simpler and more general than the RANS models. However this simplicity comes at a high price. LES must be performed on a three-dimensional grid and equations must be integrated in unsteady form, performing enough time steps to have a representative flow statistics. In this work two models are used, the Smagorinsky model, an algebraic model with only one constant to be prescribed, and the Dynamic model which uses two filters to estimate the constant in the Smagorinsky model. Hence, the Dynamic model has no adjustable constants.

1.2 Computational grid

The TOPFLOW-PTS test facility was designed to simulate the EDF CPY 900 MWe PWR. The geometrical configuration of the test facility was scaled and simplified to an extent, to allow for easier placement of instrumentation and easier interpretation of the results. According to the design of the test facility the CFD model contained the pump simulator where the hot water enters (PS), the cold leg with the emergency core cooling (ECC) inlet line and the downcomer (DC) where the fluid flows down and out of the domain, as illustrated in Figure 1. The corresponding CAD model was built with Autodesk Inventor software [15].

The computational grid was generated with ICEM CFD software. The entire computational domain was covered with approximately 850,000 hexahedral cells. The averaged value of y+ was around 400. Best practice guidelines [16] were followed as far as it was practical. The grid was prepared by the HZDR team.

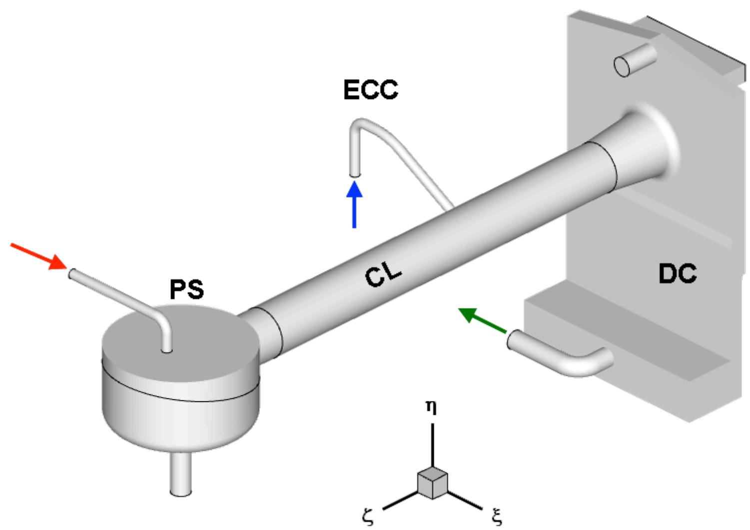

Figure 1 CAD model of the TOPFLOW PTS facility.

1.3 Boundary and initial conditions

The operating pressure in the experiment is 2.25 MPa. Boundary conditions are defined as follows. Water level was at the half height of the cold leg, and was kept constant during the simulation. The ratio of inlet PS to ECC mass flow rates was 1:1.7. The inlet temperatures at both inlets were below saturation for the working pressure, with ECC temperature (T_{ECC}) being below the temperature of PS (T_{PS}). In order to keep the water level constant, the outlet mass flow rate, at the bottom of the downcomer, was equal to the sum of the inlet mass flow rates. In the back side of the downcomer there is an opening connected to the ambient environment of the TOPFLOW vessel. The perfectly mixed temperature (T_{PS} +1.7 T_{ECC})/2.7 was set there. The exact values of temperatures, working pressure and mass flow rates are not given for confidentiality agreement with the TOPFLOW consortium.

Inlet boundary conditions, with flat velocity profiles, were prescribed at the inlet legs of the PS and the ECC. For the RANS simulations, a turbulent intensity of 5% was set at the inlet. An outlet boundary condition was set at the bottom of the downcomer. The mass flow rate is equal to the sums of inlet mass fluxes by default in FLUENT, so no values had to be specified there. Unfortunately, the opening at the top of the downcomer could not be modeled as another outlet in FLUENT, so we set it to be a wall at perfectly mixed temperatures.

All the simulations have been performed in unsteady mode. Initial velocity was zero everywhere, and initial temperature was set to the perfectly mixed one of $(T_{PS} + 1.7\ T_{ECC})/2.7$. Physical properties are kept constant in reported simulations. For all considered models, the simulation was run for 300 s, to let the flow fully develop. For RANS simulations, results are reported for the 270 s, whereas for LES, 270 s was the time when statistics started to be gathered. The LES simulations were gathered until 390 s, i.e. for two minutes of physical time. The time step for RANS simulations was Δt=1e-3 s, while it was Δt =1e-4 s for LES. Thus the time step for the RANS simulations was ten times higher than for LES, but the number of inner iterations needed was also bigger, resulting in CPU times comparable to that of LES. The total compuational time for the (unstedy) RANS simulations about 2 months wall-clock time 4 Intel Xeon CPUs at 3 GHz, while the LES simulations took 3 months wall clock time on the same machine.

2. Results

This section gives the comparison of results computed with RANS and LES approaches, with experimental findings. In all the plots presented in this section, geometrical dimensions are scaled by the cold leg diameter: $\xi = x/D$, $\eta = y/D$, $\zeta = z/D$, while the temperature is reported in its non-dimensional form: $\theta = (T - T_{ECC})/(-T_{PS} - T_{ECC})$.

2.1 General temperature and flow pattern

Flow and temperature patterns are illustrated in vertical mid-plane of the cold leg, in Fig. 2. Colours in Fig. 2 are temperatures, and dotted line is the interface between air and water. Hot water enters the facility from the upper leg of the PS, hits the inner plate structure, and is transported to the water surface. The hot water from PS heats the left part of the cold leg. Cold water is introduced through ECC (not shown in Fig. 2). The position of the ECC entry can be identified by the position of the coldest (blue) spot in the cold leg. Cold water from the ECC mixes with hot water in the leg, and flows towards the downcomer. It is interesting to note that the two streams are already well mixed before entering the downcomer.

2.2 Temperature profiles in the cold leg

Computed temperature profiles in the cold leg, for all considered turbulence models, are given in Figures 3-6. Only the temperature in the water is shown. The grey line at the bottom of the graphs represents the cold leg lower wall, whereas the dotted line on the top of the graphs is the water level.

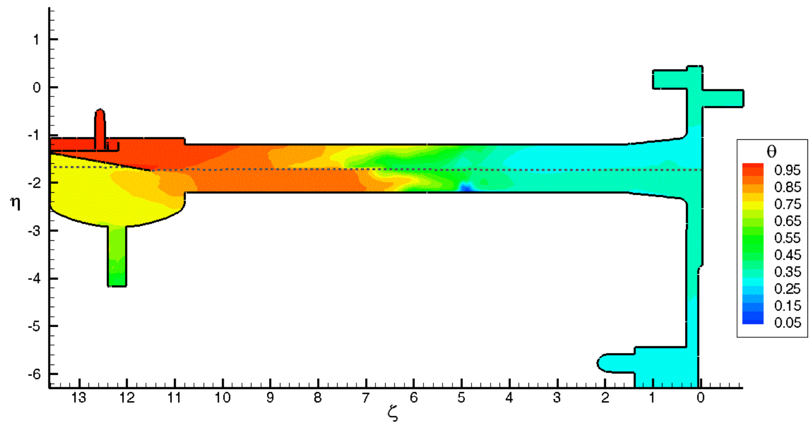

Figure 2 Simulated temperature contours (colours) and air-water interface (dashed line) in the vertical mid-plane of the facility.

HZDR carried out the temperature measurements, which were done with thermocouples. The positions of the thermocouple lines are shown in the small sketch on the left side of each figure. For comparison, the computed temperatures were taken at the same positions.

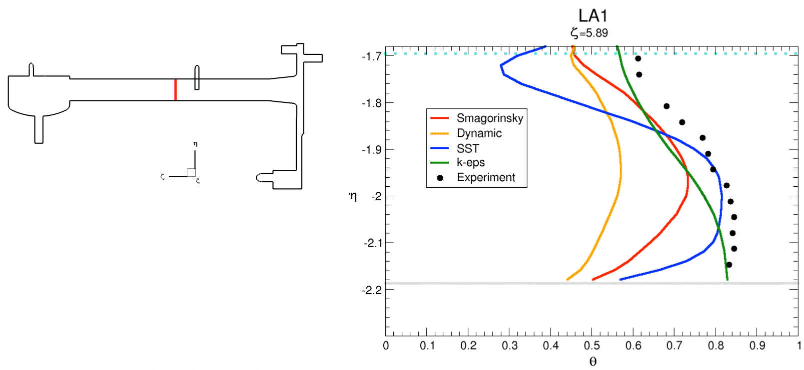

Figure 3 Location (left) and temperature profiles (right) at the thermo-couple line LA1.

The figures show a large dependency of the results on the turbulence model used. The discrepancy between the results is best visible at thermocouple line LA1 (Fig. 3). All models, except the k-ε, failed to predict the temperature at the wall and at the water surface. Both LES models fail to predict the near-wall temperature by up to 0.4. Smagorinsky predicts the bulk temperature better than Dynamic model. SST shows probably the worst comparison of all models, failing to predict the water surface temperature and the near-wall temperature. The next thermocouple line, LA2, placed after the ECC line, was easier to predict for all considered models, as shown in Fig. 4. Discrepancies in computed results are never higher than 0.1. Even at this location k-ε is closest to experiment, Smagorinsky performs better than Dynamic. The SST model shows two local extrema, which is not picked by other models.

In Figs. 5 and 6 the comparison between measured and computed results of the models further downstream in the cold leg is shown. The locations are LA4 and LA3 respectively. All models, except the SST, predict the temperature well here. Closest to the experiment is presumably the LES with Smagorinsky model.

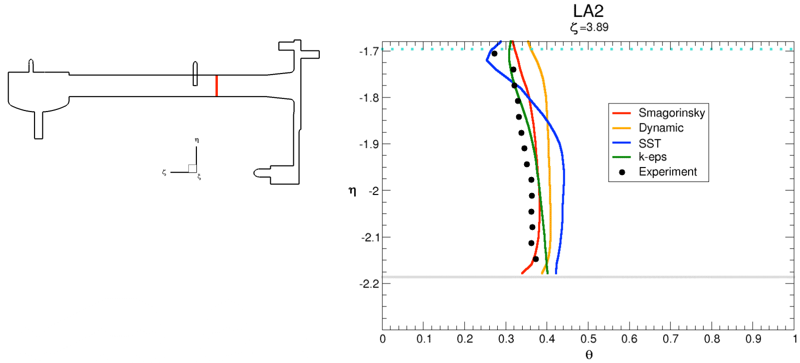

Figure 4   Location (left) and temperature profiles (right) at the thermo-coupe line LA2.

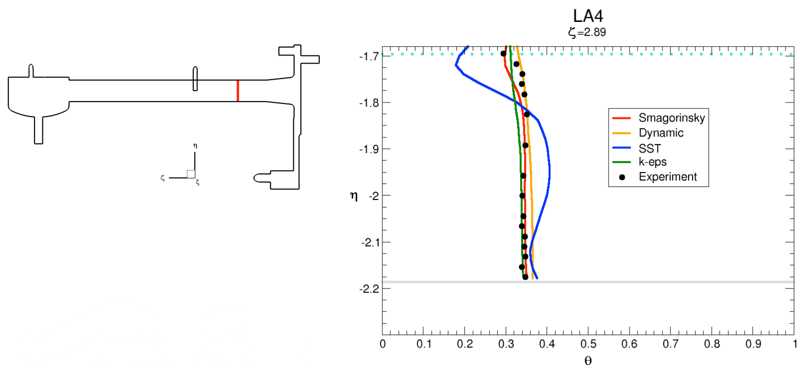

Figure 5   Location (left) and temperature profiles (right) at the thermo-coupe line LA4.

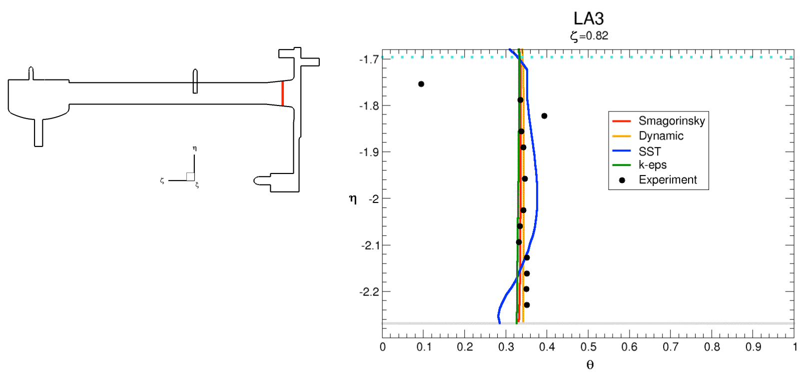

Figure 6   Location (left) and temperature profiles (right) at the thermo-coupe line LA3.

The discrepancy in computed results shown in this section is not comforting. At this level of grid refinement (i.e. with a relatively coarse mesh) the difference between k-ε and SST should be small, as the SST would be expected to work in k-ε "mode". In addition, convergence for the SST was never quite reached, and computed profiles oscillated around the reported values by several percent. At present, the differences between SST and k-ε can be attributed either to lack of robustness of the SST model, failing to reach a steady state, or the over-reaction of the SST's production limiter at the cold water injection. These issues need further investigations.

The difference between two large eddy simulations should have been smaller too. The effects of dynamic modelling procedure in LES should be notable in well-resolved, near wall regions and transition modelling. A possible explanation could lie in the underestimation of eddy viscosity at the free surface, preventing the heat-up of the liquid phase.

2.3 Temperature profiles in the downcomer

Figures 7-9 show the comparison of computed temperatures, with all considered models, with measurements, in the downcomer. Three characteristic thermocouple lines were picked, at varying depths in the downcomer. As the fluid is already well mixed at the entrance to the downcomer, temperature profiles are flat, owing to small temperature variations.

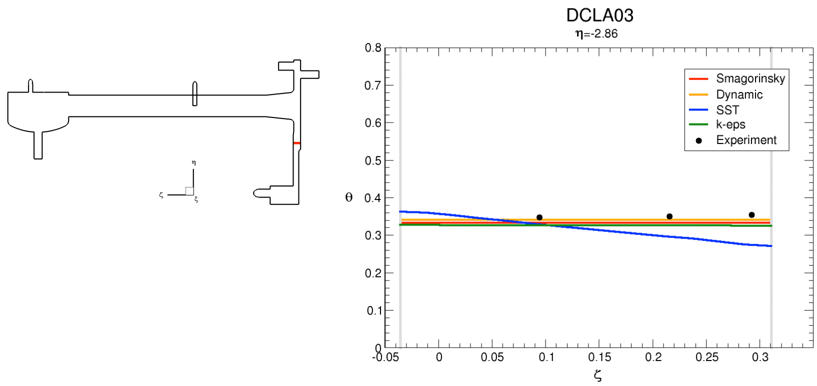

Figure 7 Location (left) and temperature profiles (right) at the thermo-coupe line DCLA03.

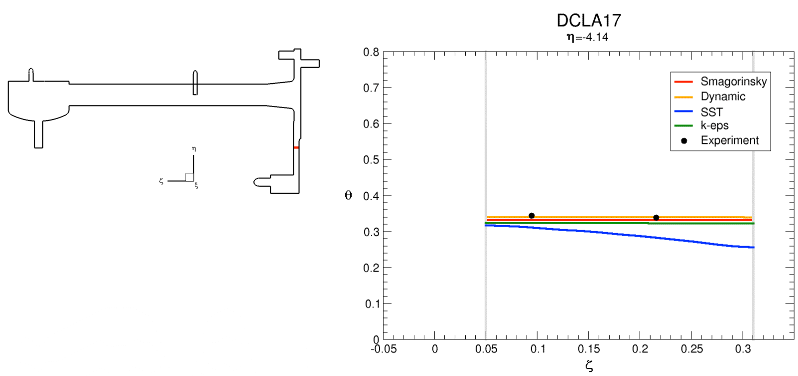

Figure 8 Location (left) and temperature profiles (right) at the thermo-coupe line DCLA17.

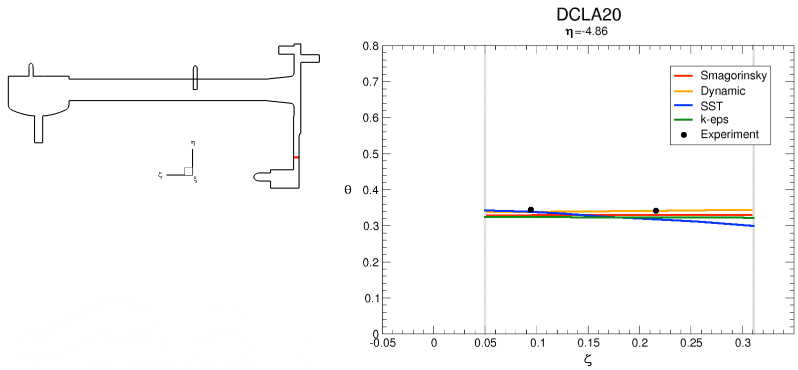

Figure 9   Location (left) and temperature profiles (right) at the thermo-coupe line DCLA20.

All models, except the SST, managed to predict the temperature profiles well. As it was mentioned above, it was difficult to obtain convergence for SST model, that might explain the poor comparison of the SST model with experiments.

3. Concluding Remarks

Simulations of the steady air-water reference test in the TOPFLOW-PTS facility are reported. The multiphase situation was modelled by the VOF approach. The influence of different turbulence models, which was the main focus of this work, was studied by applying two RANS and two LES models. For the RANS approach a k-ε and a SST model were used. For LES, a Smagorinsky and a Dynamic model were considered. All simulations, RANS and LES were conducted in unsteady mode. The time step for RANS simulations was ten times higher than for LES, but the number of inner iterations needed was also bigger, resulting in CPU times comparable to that of LES.

The general flow pattern, observed in vertical mid-plane of the cold leg, reveals that hot and coldwater streams are well mixed before reaching the downcomer. Comparison of computed temperature profiles with thermocouple line measurements showed big influence of the turbulence model used on the computed result. Surprisingly, the best overall comparison with experimental data was observed for the k-ε model, whereas the SST proves to be the worst. LES predictions with both Smagorinsky and Dynamic model are worse than the k-ε model, but better than SST. These conclusions give rise to some doubts, as less sophisticated models yield better results than more elaborate ones. A more elaborate assessment of the model performance is needed.

Acknowledgments

This work has been partially funded by European Commission in the framework of the NURISP project, which is gratefully acknowledged.

4. References

[1] NURESIM website: www.nuresim.com

[2] Bonnetto, F., Lahey Jr., R.T., "An experimental study on air carry-under due to a plunging liquid jet", International Journal of multiphase Flow, 19, pp. 1993, 281-294.

[3] Iguchi, M., Okita, K., Yamamoto, F., "Mean velocity and turbulence characteristics of water flow in the bubble dispersion region induced by plunging water jet", Int. J. Multiphase Flow, 24, 1998, pp. 523-537.

[4] Lim, I. S., Tankin, R. S., Yuen, M. C., "Condensation measurement of horizontal co-current steam-water flow", Journal of Heat Transfer, 106, pp. 1984, 425-432

[5] Vallée, C., Höhne, T., Prasser, H.-M., Sühnel, T., "Experimental investigation and CFD simulation of air/water flow in a horizontal channel", The 11th International Topical Meeting on Nuclear Reactor Thermal-Hydraulics (NURETH-11), Avignon, France, 2005.

[6] Lucas, D.; Bestion, D.; Bodèle, E.; Coste, P.; Scheuerer, M.; D'Auria, F.; Mazzini, D.; Smith, B.; Tiselj, I.; Martin, A.; Lakehal, D.; Seynhaeve, J.-M.; Kyrki-Rajamäki, R.; Ilvonen, M.; Macek, J., "An Overview of the Pressurized Thermal Shock Issue in the Context of the NURESIM Project", Science and Technology of Nuclear Installations, Volume 2009, 2009, Article ID 583259.

[7] Lucas, D.; Bestion, D.; Coste, P.; Pouvreau, J.; Morel, Ch.; Martin, A.; Boucker, M.; Bodele, E.; Schmidtke, M.; Scheuerer, M.; Smith, B.; Dhotre, M. T.; Niceno, B.; Lakehal, D.; Galassi, M. C.; Mazzini, D.; D'Auria, F.; Bartosiewicz, Y.; Seynhaeve, J.-M.; Tiselj, I.; ŠTrubelj, L.; Ilvonen, M.; Kyrki-Rajamäki, R.; Tanskanen, V.; Laine, M.; Puustinen, J., "Main results of the European project NURESIM on the CFD-modelling of two-phase Pressurized Thermal Shock (PTS)", Kerntechnik, 74, 2009, pp. 238-242.

[8] Peturaud, P. et. Al., "A general overview of the TOPFLOW PTS experimental program", The 14th International Topical Meeting on Nuclear Reactor Thermal-Hydraulics (NURETH 14) Toronto, Canada, 2011, September 25-30.

[9] Štrubelj, L., Tiselj, I., "Numerical modelling of condensation of saturated steam on subcooled water surface in horizontally stratified flow", The 12th International Topical Meeting on Nuclear Reactor Thermal Hydraulics (NURETH-12), Sheraton Station Square, Pittsburgh, Pennsylvania, U.S.A. 2007, September 30-October 4.

[10] Coste, P., Laviéville, J., Pouvreau, J., Boucker, M., "A two-phase CFD approach to the PTS problem evaluated on COSI experiment", Proc. The 16th International Conference on Nuclear Engineering ICONE16, Orlando, Florida, USA, 2008, May 11-15.

[11] Egorov, Y., "Validation of CFD codes with PTS-relevant test cases", 5th Euratom Framework Programme ECORA project, 2004.

[12] Apanasevich, P., Lucas, D. and Hohne, T., "Pre-test CFD simulations of TOPFLOW-PTS Experiments with ANSYS CFX 12.0", CFD4NRS-3, Workshop on Experimental Validation and Application of CFD and CMFD Codes to Nuclear Reactor Safety, Washington D.C., USA, 2010, September 14-16.

[13] Méchitoua, N., Boucker, M., Laviéville, J., Hérard, J., Pigny, S., and Serre, G., "An unstructured finite volume solver for two-phase water/vapour flows modelling based on an elliptic oriented fractional step method," The 10th International Topical Meeting on Nuclear Reactor Thermal-Hydraulics (NURETH 10) Seoul, Korea, 2003, October 5-9.

[14] ANSYS CFX 12 User Manual, ANSYS

[15] ANSYS FLUENT 12 User Manual, ANSYS

[16] Autodesk Inventor 2009 User Manuel, 2009, Autodesk

[17] Menter, F., „CFD Best Practice Guidelines for CFD Code Validation for Reactor Safety Applications“, ECORA FIKS-CT-2001-00154